

# Controlling phase diagram of finite spin-1/2 chains by tuning boundary interactions

Shi-Ju Ran,<sup>1</sup> Cheng Peng,<sup>2</sup> Gang Su,<sup>2,3</sup> and Maciej Lewenstein<sup>1,4</sup>

<sup>1</sup>ICFO-Institut de Ciències Fotoniques, The Barcelona Institute of Science and Technology, 08860 Castelldefels (Barcelona), Spain

<sup>2</sup>CAS Key Laboratory for Vacuum Physics, School of Physics,

University of Chinese Academy of Sciences, P. O. Box 4588, Beijing 100049, China

<sup>3</sup>Kavli Institute for Theoretical Sciences, University of Chinese Academy of Sciences, Beijing 100190, China

<sup>4</sup>ICREA, Pg. Lluís Companys 23, 08010 Barcelona, Spain

For a quantum chain or wire, it is challenging to control or even alter the bulk properties or behaviors, for instance a response to external fields by tuning solely the boundaries. This is expected, since the correlations usually decay exponentially, and do not transfer the physics at the boundaries to the bulk. In this work, we construct a quantum spin-1/2 chain of finite size, termed as controllable spin wire (CSW), in which we have  $\hat{S}^z\hat{S}^z$  (Ising) interactions with a transverse field in the bulk, and the  $\hat{S}^x\hat{S}^z$  and  $\hat{S}^z\hat{S}^z$  couplings with a canted field on the boundaries. The Hamiltonians on the boundaries, dubbed as tuning Hamiltonians (TH's), bear the same form as the effective Hamiltonians emerging in the so-called “quantum entanglement simulator” (QES) that mimics infinite models. We show that by tuning the TH's, the CSW surprisingly exhibits two different types of behaviors in response to the transverse field in the bulk. In one case, the staggered magnetization  $M_z^s$  of the bulk exhibits a steep cliff, and the entanglement entropy  $S$  shows a high peak. In the other case, no cliff or peak of  $M_z^s$  and  $S$  exists. We show that the behaviors of the CSW can be switched between these two types by solely tuning the TH's on the boundaries. The CSW could potentially serve as the basic building blocks of quantum devices for quantum sensing, quantum memories, or quantum computers. The CSW contains only nearest-neighbor spin-1/2 interactions, and could be realized in future experiments with atoms/ions coupled with artificial quantum circuits or dots.

PACS numbers: 75.78.Cd, 05.45.Pq, 85.35.Be

Quantum mechanics often leads to exotic behaviors and features that violate the common senses of the classical world. One of the central topics in modern science is investigating how to utilize the quantum features to build functional devices for the tasks that cannot be accessed, or efficiently solved by classical ones. Paradigm examples include simulating complicated quantum systems, or solving the NP-hard problems. As Feynman proposed in the American Society Meeting in 1956, “When we get to the very, very small world we have a lot of new things that would happen that represent completely new opportunities for design”.

Many efforts have been made towards this aim. One distinguished example concerns quantum simulators (cf. [1–4], for the very recent achievements see [5]), which are controllable quantum systems for efficiently mimicking the properties of other more complicated quantum systems. Another more universal proposal concerns quantum computers [6, 7], which are expected to accelerate the exponentially expensive computations to be with only polynomial costs.

Rapid development in experimental techniques provides increasing possibility of and feasibility for realizing novel functional quantum devices. For instance, cold/ultracold atoms in optical lattices or trapped ions [8, 9] allow to realize few-body models with designed interactions. Impressive results have been achieved using such methods to simulate many-body phenomena [10] including ground-state phase transitions [11], and/or dynamical processes [12] of large quantum lattice models.

However, for practical implementations of quantum devices there is still a long road to go: the proposals that can practically be realized in experiments are rare, and problems that

can be solved by existing quantum devices in a more efficient manner than by the classical ones are also severely rare. Thus, searching for simple quantum models for realizing non-trivial simulations in experiments is highly desired.

Recently, the “quantum entanglement simulators” (QES's) were proposed [13]; these are few-body models that mimic optimally the ground states of the corresponding many-body systems of infinite size. A QES is formed by two parts: bulk and boundaries. The bulk is a finite-size super-cell of the infinite model to be simulated. The Hamiltonians on the boundaries give the optimal effective interactions between the boundary physical sites and entanglement-bath sites. These effective Hamiltonians are determined by the *ab-initio* optimization principle (AOP) scheme [14, 15]; they mimic optimally the entanglement between the finite bulk and the infinite environment, allowing for optimal determination of the ground state of the infinite system.

In this work, we construct a one-dimensional (1D) spin-1/2 model of finite size, dubbed as controllable spin wire (CSW), where we have Ising interactions with a transverse field in the bulk, and the designed Hamiltonians (dubbed as the tuning Hamiltonians, TH's in short) for tuning on the boundaries. Here, the TH's have the same form as the effective physical-bath Hamiltonians emerging in the QES for simulating infinite quantum Ising chain, and are nothing but two-body nearest-neighbor spin-1/2 Hamiltonians with  $\hat{S}^x\hat{S}^z$  and  $\hat{S}^z\hat{S}^z$  interactions in a canted magnetic field [Eq. (4)]. We show that the CSW exhibits non-trivial properties that could be utilized to build functional quantum devices.

- Not only the state, but also the response of the bulk to a magnetic field can be dramatically altered by tuning

TH's on the boundaries only. It means that the ‘‘landscape’’ of the ground-state properties of the CSW can be remotely controlled from the boundaries, and thus could be used for building quantum devices. We stress that without the TH's, one has to tune the magnetic field in the whole bulk to alter the properties of the system.

- It only requires a small size ( $\mathcal{O}(10)$  sites) and an extremely weak strength of the TH's ( $\sim \mathcal{O}(10^{-2})$  of the energy scale) to fully possess the above controlling function of the CSW.
- The interactions in the bulk are only the Ising couplings (fixed) in a uniform transverse field, thus could be easily realized with, e.g., ultracold atoms or ions [16–21]; the TH's on the boundaries contain simply two-body interactions of nearest-neighboring spin-1/2's, and could be realized and tuned, for instance, by using super-lattices and ultracold atoms, ions in microtraps, quantum circuits or quantum dots coupled through photons with the bulk [8, 22–25].

*Hamiltonian of the controllable spin wire.*— The Hamiltonian of our CSW with  $N$  spin-1/2's reads

$$\hat{H} = \hat{H}_{Bulk} + \hat{H}_L + \hat{H}_R. \quad (1)$$

$\hat{H}_{Bulk}$  is the bulk Hamiltonian of the  $(N - 2)$  spins in the middle, with the interactions that are the nearest-neighbor Ising couplings in an uniform transverse field. It reads

$$\hat{H}_{Bulk} = \sum_{n=2}^{N-2} \hat{S}_n^z \hat{S}_{n+1}^z - h_{Bulk} \sum_{n=2}^{N-1} \hat{S}_n^x. \quad (2)$$

The  $\hat{S}^z \hat{S}^z$  coupling constant multiplied by the Planck constant  $\hbar$  is set to be one, so that it defines the energy unit. Without losing generality, we take  $N$  to be even.

$\hat{H}_L$  and  $\hat{H}_R$  are the TH's, which include the interactions between the first two and the last two sites, respectively. These Hamiltonians bear the same form as the effective Hamiltonians emerging in the QES [13]. The QES is obtained by the AOP approach [13, 14], and is a few-body model that optimally mimics the ground state of the infinite system. In this work, we take the TH's in the QES of the infinite transverse Ising model, whose Hamiltonian reads

$$\hat{H}_{Inf} = \sum_n [\hat{S}_n^z \hat{S}_{n+1}^z - \frac{\alpha}{2} (\hat{S}_n^x + \hat{S}_{n+1}^x)], \quad (3)$$

where  $\alpha$  is a uniform transverse field in the  $x$  direction, and the summation runs over the infinite chain.

A QES contains  $\tilde{N}$  sites with  $\tilde{N}$  a finite number, where the first and the last sites are called bath sites. The TH's on the boundaries of the QES are optimized, so that the reduced density matrix of the  $(\tilde{N}-2)$  spins in the bulk of the QES optimally approximates the  $\tilde{N}$ -site reduced density matrix of the infinite model. Thus, the TH's are originally the effective Hamiltonians for simulating infinite models. In this work, we take the

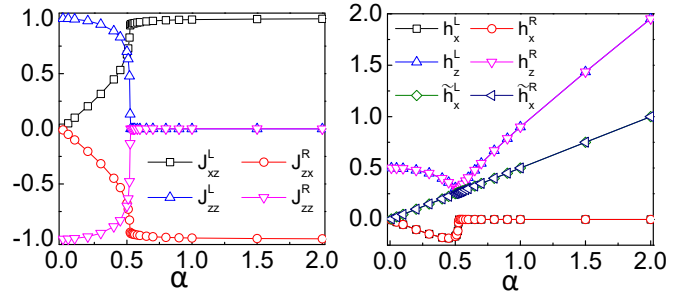


Figure 1: (Color online) The  $\alpha$ -dependence of the coupling constants (left) and magnetic fields (right) of the tuning Hamiltonians [Eq. (4)].

bath dimension as  $\dim(bath) = 2$ , and use the TH's as physical Hamiltonians of spin-1/2's. The detail of the algorithm can be found in the Appendix, as well as Refs. [13–15]. After determining the TH's, we study the ground state of the Hamiltonian of the CSW in Eq. (1) by the exact diagonalization and finite-size density matrix renormalization group algorithm [26].

*Parameterizing the tuning Hamiltonians.*— Since the TH's are from the QES, designed for simulating an infinite Ising chain, the transverse field  $\alpha$  is a good choice as the control parameter of the TH's. The AOP simulation shows that  $\hat{H}_L$  and  $\hat{H}_R$  simply contain  $\hat{S}^x \hat{S}^z$  and  $\hat{S}^z \hat{S}^z$  couplings in a canted magnetic field as

$$\begin{aligned} \hat{H}_L &= J_{xz}^L \hat{S}_1^x \hat{S}_2^z + J_{zz}^L \hat{S}_1^z \hat{S}_2^z - h_x^L \hat{S}_1^x - h_z^L \hat{S}_1^z - \tilde{h}_x^L \hat{S}_2^x, \\ \hat{H}_R &= J_{xz}^R \hat{S}_{N-1}^x \hat{S}_N^z + J_{zz}^R \hat{S}_{N-1}^z \hat{S}_N^z - h_x^R \hat{S}_N^x - h_z^R \hat{S}_N^z - \tilde{h}_x^R \hat{S}_{N-1}^x. \end{aligned} \quad (4)$$

Except the Ising interactions and the transverse field that originally appear in the infinite model, the  $\hat{S}^x \hat{S}^z$  coupling and a vertical field emerge in the TH's. This is interesting, because the  $\hat{S}^x \hat{S}^z$  interaction is the stabilizer on the open boundaries of the cluster state, a highly entangled state that has been widely used in quantum information sciences [27, 28]. More relations with the cluster state are to be further explored.

Firstly, one can see that in the TH's, there are the magnetic fields  $\tilde{h}_x^L$  and  $\tilde{h}_x^R$  on the second and the last second spins, respectively. Though these two terms are in  $\hat{H}_L$  and  $\hat{H}_R$ , they in fact belong to  $\hat{H}_{Bulk}$ .  $\hat{H}_L$  and  $\hat{H}_R$  are calculated from the infinite Hamiltonian  $\hat{H}_{Inf}$  in Eq. (3). To explicitly obey the translational invariance,  $\hat{H}_{Inf}$  is written as the summation of two-body terms, where the one-body terms (the magnetic fields) are put inside. By taking a finite part of the infinite chain, one can see that the magnetic fields on both ends of the finite part is only half of the field on the other sites. Interestingly, this missing field automatically appears in  $\hat{H}_L$  and  $\hat{H}_R$ , making the field uniform again. Our calculation confirms that  $\tilde{h}_x^L = \tilde{h}_x^R = \alpha/2$  with an error smaller than the machine error. In the following, we remove these fields from  $\hat{H}_L$  and  $\hat{H}_R$ , and ensure that the field on all  $(N - 2)$  sites in the bulk of the CSW is uniformly  $h_{Bulk}$ .

Due to the symmetry of the infinite chain, we have

$$\begin{aligned} J_{xz}^L &= -J_{xz}^R \doteq \bar{J}_{xz}, & J_{zz}^L &= -J_{zz}^R \doteq \bar{J}_{zz}, \\ h_x^L &= h_x^R \doteq \bar{h}_x, & h_z^L &= h_z^R \doteq \bar{h}_z, & \tilde{h}_x^L &= \tilde{h}_x^R \doteq \tilde{h}_x. \end{aligned} \quad (5)$$

One can see that the coupling constants have the odd parity and the magnetic fields have the even parity, when changing from the left to the right boundary. This is because the couplings in the transverse Ising model is antiferromagnetic, and the magnetic field is uniform. Interestingly, changing the sign of  $\bar{h}_x$  or  $\bar{J}_{zz}$  does not affect the results.

The  $\alpha$ -dependences of the coupling constants and magnetic fields in  $\hat{H}_L$  and  $\hat{H}_R$  are given in Fig. 1. Note that the Hamiltonian of the CSW is given by Eq. (1), and  $\alpha$  only plays the role of a control parameter that has one-to-one correspondence with the coupling constants and fields of the TH's. In the following, we will tune the TH's by tuning  $\alpha$ .

Let us take some limits of  $\alpha$  to see how the values of the coupling constants in Eq. (5) change. As shown in Fig. 1, for  $\alpha \rightarrow \infty$  we have  $\bar{J}_{xz} \rightarrow 1$ ,  $\bar{J}_{zz} \rightarrow 0$ ,  $\bar{h}_x \rightarrow 0$ , and  $\bar{h}_z \rightarrow \alpha$ . It means that in this limit, the TH's become the  $\hat{S}^x \hat{S}^z$  coupling in a vertical field (in the  $z$  direction). For  $\alpha \rightarrow 0$ , we have  $\bar{J}_{xz} \rightarrow 0$ ,  $\bar{J}_{zz} \rightarrow 1$ ,  $\bar{h}_x \rightarrow 0$ , and  $\bar{h}_z \rightarrow 0.5$ . The boundary interactions become the Ising coupling in a fixed vertical field. This leads exactly to the  $N$ -site classical Ising chain in a mean field.

Moreover, singular behaviors of the constants and fields are found near  $\alpha = \alpha^s = 0.5$ . Interestingly,  $\alpha = 0.5$  is in fact the critical point of the infinite transverse Ising chain [Eq. (3)]. In the following, we will show that  $\alpha^s = 0.5$  is a ‘‘switch point’’ where a dramatical change of the landscape of the ground-state properties occurs.

*Controlling the bulk by tuning the interactions on the boundaries.*— Let us take  $\alpha$  as the control parameter, and simulate how the CSW responds to the magnetic field  $h_{Bulk}$  in the bulk. We discover that with the presence of the TH's, the ground state exhibits essentially different properties compared with a finite transverse Ising chain. Fig. 2 shows the  $\alpha$ -dependence of the energy spectrum  $E(n)$  and the logarithmic ground-state entanglement spectrum  $\ln \lambda_n$  of the CSW with different  $h_{Bulk}$ . The entanglement is measured in the middle of the chain. With small  $h_{Bulk}$ , e.g.,  $h_{Bulk} = 0.1$ , the ground state has two-fold degeneracy for  $\alpha > 0.5$  with the difference between the two lowest energies around  $O(10^{-7})$ . In this region, the entanglement spectrum show some instability. The reason might be that the super-position of the degenerate states does not robustly leads to a unique entanglement.

At  $h_{Bulk} = 0.2$ , the degeneracy of the ground state still exists with the energy difference around  $O(10^{-5})$ . Meanwhile, the entanglement is stabilized and the two leading Schmidt numbers become degenerate with a difference around  $O(10^{-2})$ . As  $h_{Bulk}$  becomes larger, e.g.,  $h_{Bulk} = 0.3$  and  $0.4$ , the differences increases, destroying the degeneracy of both the energy and entanglement spectrums. In all cases, there is no degeneracy for  $\alpha < 0.5$ . We dub  $\alpha^s = 0.5$  as the *switch point*.

To further study the switch point, in Fig. 3 (a)-(c) we show the staggered magnetization in the  $z$  direction  $M_z^s = \langle \phi | (\sum_{n=2,4,\dots,N-2} \hat{S}^z - \sum_{n=3,5,\dots,N-1} \hat{S}^z) | \phi \rangle / (N-2)$  and the entanglement entropy  $S = -\sum \lambda_i^2 \ln \lambda_i^2$ . For  $M_z^s$ , it shows two different kinds of responses to the transverse field  $h_{Bulk}$  with different  $\alpha$ . For  $\alpha > \alpha^s$ , a very steep cliff of  $M_z^s$  dropping from

Table I: The fidelity  $F = |\langle \phi' | \phi \rangle|$  between the ground states of two Hamiltonians that have different signs of  $\bar{h}_x$  and  $\bar{J}_{zz}$  in the TH's. We take  $L = 8$ ,  $\alpha = 0.3$  and  $h_{Bulk} = 0.3$ . The ground states of the Hamiltonians with opposite signs of  $\bar{J}_{zz}$  have the same properties, but are orthogonal to each other, giving a vanishing fidelity  $F \sim O(10^{-5})$ .

$\bar{h}_x/\bar{J}_{zz}$	+/+	+/-	-/+	-/-
+/+	1	$3.9(2) \times 10^{-5}$	0.97(5)	$4.3(8) \times 10^{-5}$
+/-	$3.9(2) \times 10^{-5}$	1	$2.99 \times 10^{-5}$	0.97(5)
-/+	0.97(5)	$2.99 \times 10^{-5}$	1	$3.9(2) \times 10^{-5}$
-/-	$4.3(8) \times 10^{-5}$	0.97(5)	$3.9(2) \times 10^{-5}$	1

a large value ( $\simeq 0.5$ ) to zero appears around  $h_{Bulk}^c = 0.2$ . It means that in this region, the staggered magnetic order parameter behaves similarly to the quantum phase transition from the Néel phase to polarized phase. Similar behaviors are found for the entanglement entropy  $S$  for  $\alpha > 0.5$ , which reaches its maximum around  $h_{Bulk}^c = 0.2$ . For comparison,  $M_z^s$  and  $S$  only change smoothly with  $h_{Bulk}$ .

For the ground-state uniform magnetization in the  $x$  direction  $M_x^u = \langle \phi | \sum_{n=2}^{N-1} \hat{S}^x | \phi \rangle / (N-2)$ , we find no singular behaviors in the whole  $h_{Bulk}$ - $\alpha$  region (see the supplementary material). With a fixed  $h_{Bulk}$ ,  $M_x^u$  changes very slowly when tuning  $\alpha$ . It means that the boundary interactions do not have much effects on  $M_x^u$  in the bulk.

The peak of  $S$  is due to the two-fold degeneracy of the entanglement spectrum shown in Fig. 2, thus can be the indicator of the degeneracy. Then, one can see that at  $h_{Bulk} = h_{Bulk}^c$ , the leading Schmidt numbers are stabilized and the difference between them reaches the minimum. Meanwhile, the two lowest energies remain degenerate at this point. As  $h_{Bulk}$  continues increasing, both spectra start to split.

Amazingly, for  $\alpha < \alpha^s$ , we discover that the ‘‘degeneracy’’ is hidden behind the signs of  $\bar{J}_{zz}$  in the TH's. Note that changing the signs of  $\bar{h}_x$  and  $\bar{J}_{zz}$  do not affect the ground-state properties, thus we calculate the fidelity to compare the ground states. For  $\alpha < 0.5$ , the ground state of the Hamiltonian does not possess any degeneracy whatever the sign of  $\bar{h}_x$  or  $\bar{J}_{zz}$  is. If we change the sign of  $\bar{J}_{zz}$ , the new ground state is orthogonal to the one before changing the sign. Changing the sign of  $\bar{h}_x$  does not affect anything. See the fidelity in Table I. Thus in this case, the two Hamiltonians with different signs of  $\bar{J}_{zz}$  have exactly the same ground-state properties, but their ground states are orthogonal to each other. For  $\alpha > \alpha^s$  for comparison, the Hamiltonian has degenerate ground states, and changing the sign of  $\bar{h}_x$  or  $\bar{J}_{zz}$  does not make any difference to the ground states. Our results show that the two orthogonal ground states can be controlled by the sign of  $\bar{J}_{zz}$  in the TH's.

We shall stress that with or without  $\alpha$ , these two different types of landscapes exist and can be reached by setting the coupling constants and fields in the TH's properly according to the numerical results shown in Fig. 1. In other words, the existence of the landscapes and the switch do not rely on the

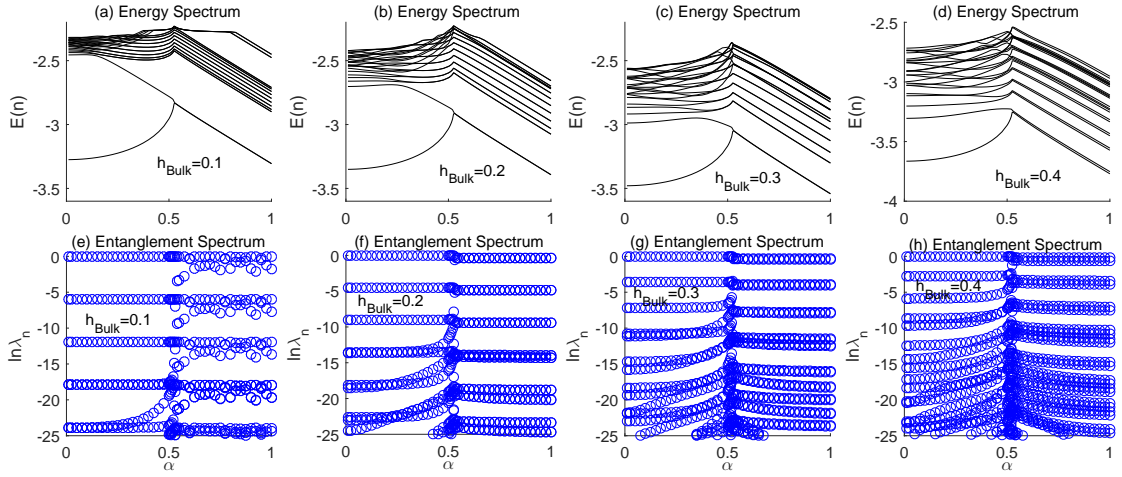


Figure 2: (Color online) The  $\alpha$ -dependence of (a)-(d) The energy spectrum and (e)-(h) the entanglement spectrum  $\lambda$  of the ground state in the middle of the CSW with different  $h_{\text{Bulk}}$ . At  $h_{\text{Bulk}} = 0.1$ , the ground-state energy has two-fold degeneracy (with a energy difference  $O(10^{-7})$ ) for  $\alpha > 0.5$ , and the two leading Schmidt numbers show certain instability. At  $h_{\text{Bulk}} = 0.2$ , The two-fold degeneracy appears for both the ground-state energy (difference  $O(10^{-5})$ ) and the entanglement spectrum (difference  $O(10^{-2})$ ). From the results of  $h_{\text{Bulk}} = 0.3$  and  $0.4$ , we see that the difference between the two-largest values of the energy or entanglement spectrum increases with the bulk field. In all cases, there is no degeneracy for  $\alpha < 0.5$ .

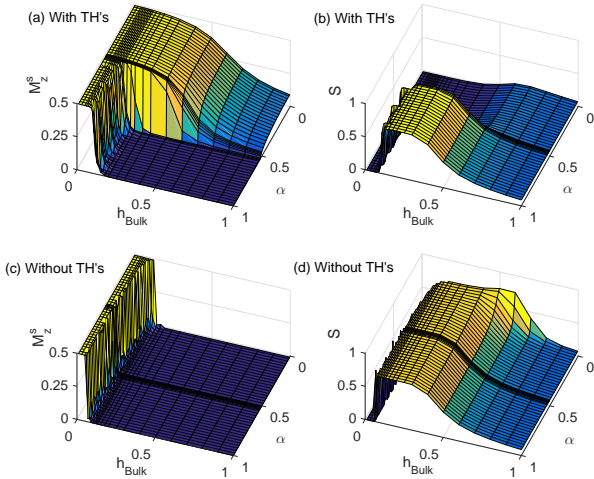


Figure 3: (Color online) (a) and (b) show the ground-state staggered magnetization in the  $z$  direction  $M_z^s$  and the entanglement entropy  $S$  with different values of the bulk transverse field  $h_{\text{Bulk}}$  and the control parameter  $\alpha$  of the TH's on the boundaries. (c) and (d) show the same quantities of the standard finite Ising chain in the transverse fields  $h_{\text{Bulk}}$  in the bulk and  $\alpha$  on the boundary sites. The magnetization is taken as the average per site inside the bulk, i.e., the  $(N-2)$  spins in the middle, and the entropy is from the bipartite entanglement in the middle of the chain. We take  $N = 12$  here.

path that how the constants and fields in the TH's are tuned or parameterized. However, if we alter the landscape by tuning the control parameter  $\alpha$ , we will have a well-defined switch point at  $\alpha^s = 0.5$ . From Fig. 1, we have  $\bar{J}_{xz} \simeq 1$ ,  $\bar{J}_{zz} \simeq 0$ ,  $\bar{h}_x \simeq 0$ , and  $\bar{h}_z \simeq 0.31$  at  $\alpha = \alpha^s$ . Comparing with the picture

of the QES for the infinite quantum Ising chain in Eq. (3), the switch point coincides with the critical point ( $\alpha = 0.5$ ) of the infinite model. Since the TH's optimally generate the entanglement bath of the infinite chain, our work implies that the remote switch of the CSW is triggered by the effects of the entanglement bath which approximately mimics the entanglement from an infinite chain.

For comparison, we implement similar numerical experiments on the finite transverse Ising chain without the TH's. The Hamiltonian simply reads  $\hat{H}_{\text{Ising}} = \sum_{n=1}^{N-1} \hat{\sigma}_n^z \hat{\sigma}_{n+1}^z - h_{\text{Bulk}} \sum_{n=2}^{N-1} \hat{\sigma}_n^x - \alpha (\hat{\sigma}_1^x + \hat{\sigma}_N^x)$ .  $h_{\text{Bulk}}$  is still the transverse field in the bulk, and  $\alpha$  here is the transverse field on the boundary sites. The results of  $M_x^u$ ,  $M_z^s$  and  $S$  are given in Fig. 3 (d)-(f). For different  $\alpha$ , the behavior of  $M_x^u$  in the bulk is similar to that with the TH's. For  $M_z^s$  and  $S$ , however, no qualitative change occurs with different  $\alpha$ , and the switch point is gone. It means that all the three quantities of the bulk hardly respond to the change of the transverse field on the boundaries. Furthermore,  $\alpha$  does not alter the degeneracy of the energy spectrum or the entanglement spectrum (see the supplementary material). Our results show that with the TH's, we are enabled to drastically alter the landscape of the bulk by only operating on the boundaries; without the TH's, one has to change the magnetic fields in the whole bulk to alter the properties of the system.

More results are given in the supplementary material to reveal the properties of the CSW. We find that the control by the TH's is robust for different sizes of the CSW and a weak coupling strength of the TH's. The controlling can be deactivated by fixing the magnetic field on the second and last second sites to be zero. The fidelity is calculated when the phase of the bulk is driven from one to another by solely tuning the TH's.

These could be useful information for the future applications of the CSW.

*Conclusions and prospects.*— In this work, we propose the controllable spin wire, with quantum Ising interactions in the bulk and the QES-inspired interactions on the boundaries. By solely tuning the interactions on the boundaries, not only the properties of the bulk of the CSW (including the ground-state degeneracy, entanglement and magnetization), but also its response to the external magnetic field can be controlled. The interactions in the CSW are simple, and the system size can be moderately small, so that the CSW could be potentially used to build practical quantum devices with controllable magnetization and entanglement, using cold-atom or cold-ion platforms.

In the future, we plan to investigate the QES-inspired Hamiltonians of non-conventionally ordered systems (e.g., the integer spin chains [29, 30]) or systems in higher dimensions. Furthermore, we will explore feasible and tunable interactions that couple multiple CSW's into size-scalable networks. We expect to be able to design and develop devices with more complicated and universal controlling properties.

*Acknowledgments.*—We acknowledge Leticia Tarruell, Ignacio Cirac, Emanuele Tirrito, Angelo Piga and Xi Chen for enlightening discussions. This work was supported by ERC AdG OSYRIS (ERC-2013-AdG Grant No. 339106), the Spanish MINECO grants FOQUS (FIS2013-46768-P), FISICATEAMO (FIS2016-79508-P), and “Severo Ochoa” Programme (SEV-2015-0522), Catalan AGAUR SGR 874, Fundació Cellex, EU FETPRO QUIC and CERCA Programme / Generalitat de Catalunya. SJR acknowledges Fundació Catalunya - La Pedrera · Ignacio Cirac Program Chair. C.P. and G. S. were supported in part by the MOST of China (Grant No. 2013CB933401), the NSFC (Grant No. 14474279), and the Strategic Priority Research Program of the Chinese Academy of Sciences (Grant No. XDB07010100).

---

[1] J. I. Cirac and P. Zoller, *Goals and opportunities in quantum simulation*, Nat. Phys. **8**, 264-266 (2012).  
 [2] I. Bloch, J. Dalibard, and S. Nascimbéne, *Quantum simulations with ultracold quantum gases*, Nat. Phys. **8**, 267 (2012).  
 [3] A. Aspuru-Guzik and P. Walther, *Photonic quantum simulators*, Nat. Phys. **8**, 285-291 (2012).  
 [4] I. M. Georgescu, S. Ashhab and Franco Nori, *Quantum simulation*, Rev. Mod. Phys. **86**, 153 (2014).  
 [5] H. Bernien, S. Schwartz, A. Keesling, H. Levine, A. Omran, H. Pichler, S. Choi, A. S. Zibrov, M. Endres, M. Greiner, V. Vuletić, M. D. Lukin, *Probing many-body dynamics on a 51-atom quantum simulator*, arXiv:1707.04344.  
 [6] T. D. Ladd, F. Jelezko, R. Laflamme, Y. Nakamura, C. Monroe and J. L. O'Brien, *Quantum computers*, Nature **464**, 45-53 (2010).  
 [7] I. Buluta, S. Ashhab and F. Nori, *Natural and artificial atoms for quantum computation*, Rep. Prog. Phys. **74**, 104401 (2011).  
 [8] M. Lewenstein, A. Sanpera, and V. Ahufinger, *Ultracold atoms in Optical Lattices: simulating quantum many body physics*,

(Oxford University Press, Oxford, 2012).  
 [9] W. S. Bakr, J. I. Gillen, A. Peng, S. Fölling and M. Greiner, *A quantum gas microscope for detecting single atoms in a Hubbard-regime optical lattice*, Nature **462**, 74-77 (2009).  
 [10] I. Bloch, J. Dalibard, and W. Zwerger, *Quantum phase transition from a superfluid to a Mott insulator in a gas of ultracold atoms*, Rev. Mod. Phys. **80**, 885 (2008).  
 [11] M. Greiner, O. Mandel, T. Esslinger, T. W. Hänsch and I. Bloch, *Quantum phase transition from a superfluid to a Mott insulator in a gas of ultracold atoms*, Nature **415**, 39 (2002).  
 [12] D. Leibfried, B. DeMarco, V. Meyer, M. Rowe, A. Ben-Kish, J. Britton, W. M. Itano, B. Jelenković, C. Langer, T. Rosenband, and D. J. Wineland, *Trapped-Ion Quantum Simulator: Experimental Application to Nonlinear Interferometers*, Phys. Rev. Lett. **89**, 247901 (2002).  
 [13] S. J. Ran, A. Piga, C. Peng, G. Su, and M. Lewenstein, *Few-Body Systems Capture Many-Body Physics: Tensor Network Approach*, arXiv:1703.09814.  
 [14] S. J. Ran, *Ab initio optimization principle for the ground states of translationally invariant strongly correlated quantum lattice models*, Phys. Rev. E **93**, 053310 (2016).  
 [15] E. Tirrito, M. Lewenstein, and Shi-Ju Ran, *Criticality and Excitation Gap in Quantum Systems: Applications of Continuous Matrix Product States in Imaginary Time*, arXiv:1608.06544.  
 [16] A. Friedenauer, H. Schmitz, J. T. Glueckert, D. Porras, T. Schaetz, *Simulating a quantum magnet with trapped ions*, Nat. Phys. **4**, 757 (2008).  
 [17] K. Kim, M. S. Chang, R. Islam, S. Korenblit, L. M. Duan, and C. Monroe, *Entanglement and Tunable Spin-Spin Couplings between Trapped Ions Using Multiple Transverse Modes*, Phys. Rev. Lett. **103**, 120502 (2009).  
 [18] K. Kim, M.-S. Chang, S. Korenblit, R. Islam, E. E. Edwards, J. K. Freericks, G.-D. Lin, L.-M. Duan, and C. Monroe, *Quantum simulation of frustrated Ising spins with trapped ions*, Nature **465**, 590593 (2010).  
 [19] R. Islam, E. E. Edwards, K. Kim, S. Korenblit, C. Noh, H. Carmichael, G. D. Lin, L. M. Duan, C. C. Wang, J. K. Freericks, et al., *Onset of a quantum phase transition with a trapped ion quantum simulator*, Nature communications **2**, 377 (2011).  
 [20] A. Khromova, C. Piltz, B. Scharfenberger, T. F. Gloger, M. Johanning, A. F. Varn, and C. Wunderlich, *Designer Spin Pseudomolecule Implemented with Trapped Ions in a Magnetic Gradient*, Phys. Rev. Lett. **108**, 220502 (2012).  
 [21] R. Islam, C. Senko, W. C. Campbell, S. Korenblit, J. Smith, A. Lee, E. E. Edwards, Wang, J. K. Freericks, and C. Monroe, *Emergence and Frustration of Magnetism with Variable-Range Interactions in a Quantum Simulator*, Science **340**, 583 (2013).  
 [22] M. H. Devoret and J. M. Martinis, *Implementing qubits with superconducting integrated circuits*, Quant. Inf. Proc. **3**, 381 (2004).  
 [23] R. J. Schoelkopf and S. M. Girvin, *Wiring up quantum systems*, Nature **451**, 664 (2008).  
 [24] J. Clarke and F. K. Wilhelm, *Review Article Superconducting quantum bits*, Nature **453**, 1031 (2008).  
 [25] M. H. Devoret and R. J. Schoelkopf, *Superconducting Circuits for Quantum Information: An Outlook*, Science **339**, 1169 (2013).  
 [26] S. R. White, *Density matrix formulation for quantum renormalization groups*, Phys. Rev. Lett. **69**, 2863 (1992); *Density-matrix algorithms for quantum renormalization groups*, Phys. Rev. B **48**, 10345 (1993).  
 [27] H. J. Briegel and R. Raussendorf, *Persistent Entanglement in Arrays of Interacting Particles*, Phys. Rev. Lett. **86**, 910 (2001).  
 [28] R. Raussendorf and H. J. Briegel, *A One-Way Quantum Com-*

- puter, Phys. Rev. Lett. **86**, 5188 (2001).
- [29] F. D. M. Haldane, *Continuum dynamics of the 1-D Heisenberg antiferromagnet: identification with the  $O(3)$  nonlinear sigma model*, Phys. Lett. A **93**, 464 (1983).
- [30] F. D. M. Haldane, *Nonlinear Field Theory of Large-Spin Heisenberg Antiferromagnets: Semiclassically Quantized Solitons of the One-Dimensional Easy-Axis *Nel* State*, Phys. Rev. Lett. **50**, 1153 (1983).

## Supplemental Material

### AB-INITIO OPTIMIZATION PRINCIPLE OF TENSOR NETWORKS

The *ab-initio* optimization principle (AOP) scheme is a tensor network (TN)-based numerical approach for simulating the ground states of infinite quantum lattice models. The idea is using Trotter-Suzuki decomposition to transform the evolution of infinite imaginary time of the model into a TN contraction problem, and then solving the TN contraction by encoding it into local self-consistent equations. Here, we take the generalized AOP approach borrowed from the infinite density matrix renormalization group algorithm, which allows to deal with non-Hermitian cases.

The Hamiltonian of infinite size is written as

$$\hat{H}_{Inf} = \sum_n \hat{H}_{n,n+1}, \quad (S1)$$

with  $\hat{H}_{n,n+1}$  the two-body interaction. We impose translational invariance here. To simulate the ground state, we firstly take a  $\tilde{N}$ -site finite bulk of the system as the supercell, say two spins with  $\tilde{N} = 2$ . The rest of the system is considered as the infinite environment. Then divide the local interactions into three parts: the ones inside the supercell  $\hat{H}_B = \hat{H}_{n,n+1}$ , those connecting the supercell and the environment  $\hat{H}_\partial = \hat{H}_{n',n'+1}$ , and those in the environment.

To obtain the TN, let us make a shift of  $\hat{H}_\partial$  as

$$\hat{F}^\partial = \hat{I} - \tau \hat{H}_\partial, \quad (S2)$$

with  $\tau$  a small number that plays the role of the Trotter-Suzuki step. This shift will not change the ground state. Introduce an ancillary particle  $a$  and rewrite  $\hat{F}_\partial$  as a sum of operators as

$$\hat{F}_\partial = \sum_a \hat{F}_L(s, a) \otimes \hat{F}_R(s', a), \quad (S3)$$

where  $\hat{F}_L(s, a)$  and  $\hat{F}_R(s', a)$  are two sets of one-body operators acting on the left and right one of the two spins associated with  $\hat{H}_\partial$ , respectively. Eq. (S3) can be easily achieved by directly rewriting Eq. (S2) or using eigenvalue decomposition.

Construct the operator  $\hat{\mathcal{F}}(S, aa')$ , with  $S = (s, s')$  representing the two physical spins in the super-cell, as

$$\hat{\mathcal{F}}(S, aa') = \tilde{H}_B \hat{F}_R(s_1, a)^\dagger \hat{F}_L(s', a), \quad (S4)$$

where one has  $\tilde{H}_B = \hat{I} - \varepsilon \hat{H}_B$ .  $\hat{F}_R(s, a)^\dagger$  and  $\hat{F}_L(s', a)$  act on the first and last sites of the super-cell, respectively. One can see that  $\hat{\mathcal{F}}(S, aa')$  contains two physical spins in the supercell and two ancillary spins ( $a$  and  $a'$ ) on the boundaries. In the language of TN, the co-efficients of  $\hat{\mathcal{F}}(S, aa')$  in the local basis is a forth-order tensor as

$$T_{ss'aa'} = \langle s | \hat{\mathcal{F}}(S, aa') | s' \rangle. \quad (S5)$$

The infinite copies of  $T$  (dubbed as cell tensor) form the TN of the imaginary-time evolution of the infinite system up to the first Trotter-Suzuki order.

To solve the TN contraction, we introduce three third-order variational tensors denoted by  $v^L$ ,  $v^R$  (dubbed as boundary tensors) and  $\Psi$  (dubbed as central tensor).  $v^L$  and  $v^R$  are, respectively, the left and right dominant eigenvectors of the following matrices

$$M_{ab_1b'_1, a'b_2b'_2}^L = \sum_{ss'} T_{ss'aa'} A_{sb_1b_2}^* A_{s'b'_1b'_2}, \quad (S6)$$

$$M_{a'b_1b'_1, ab_2b'_2}^R = \sum_{ss'} T_{ss'aa'} B_{sb_1b_2}^* B_{s'b'_1b'_2}, \quad (S7)$$

where  $A$  and  $B$  are the left and right orthogonal parts of  $\Psi$  as

$$\Psi_{sbb'} = \sum_{b''} A_{sbb''} \tilde{\Psi}_{b''b'} = \sum_{b''} \tilde{\Psi}_{bb''}^\dagger B_{sb''b'}. \quad (S8)$$

Eq. (S8) can be achieved by the QR decomposition.  $\Psi$  is the dominant eigenvector of the Hermitian matrix

$$\mathcal{H}_{sb_1b_2, s'b'_1b'_2} = \sum_{s_2s_4} T_{ss'aa'} V_{ab_1b'_1}^L V_{a'b_2b'_2}^R. \quad (S9)$$

Each of the eigenvalue problems [Eqs. (S6), (S7) and (S9)] are parametrized by the solutions of the others, thus we solve them in a recursive way. First, we initialize arbitrarily the central tensors  $\Psi$  and get  $A$  and  $B$  by Eq. (S8). Note that a good initial guess can make the simulations faster and more stable. Then we update  $v^L$  and  $v^R$  by  $v^{L\dagger} M^L$  and  $M^R v^R$ , respectively [Eqs. (S6) and (S7)]. Then we update  $\Psi$  by solving the first eigenvector of  $\mathcal{H}$  in Eq. (S9) that is defined by the new  $v^L$  and  $v^R$ . We iterate such a process until all variational tensors converge. The ground state is then given by an matrix product state formed by  $\Psi$ ,  $A$  and  $B$  as

$$|\Phi\rangle = \sum_{\{b\}} \cdots A_{s_{n-2}b_{n-2}b_{n-1}} A_{s_{n-1}b_{n-1}b_n} \Psi_{s_n b_n b_{n+1}} B_{s_{n+1}b_{n+1}b_{n+2}} B_{s_{n+2}b_{n+2}b_{n+3}} \cdots \quad (\text{S10})$$

Since  $A$  and  $B$  are orthogonal, Eq. (S10) is called central orthogonal MPS. Here, one can see that the bond dimension of  $b_n$  is in fact the dimension cut-off of the MPS

### CALCULATING THE PHYSICAL-BATH HAMILTONIANS

The ground-state properties can be calculated from the MPS. Specifically, the reduced density matrix  $\hat{\rho}_B$  of the bulk (2 spins in our example) can be calculated by tracing all other physical indexes. From the orthogonality of  $A$  and  $B$ , it can be easily seen that  $\hat{\rho}_B$  is given by the reduced matrix of  $\Psi$  by tracing all virtual bonds as

$$\hat{\rho}_B = \sum_{s_1 s_2 s'_1 s'_2} \left( \sum_{bb'} \Psi_{s'_1 s'_2 bb'}^* \Psi_{s_1 s_2 bb'} \right) |s'_1 s'_2\rangle \langle s_1 s_2|. \quad (\text{S11})$$

In other words, the reduced matrix of  $\Psi$  optimally gives that of the infinite ground states. Interestingly,  $\Psi$  is just the ‘‘ground state’’ of  $\hat{\mathcal{H}}$ , which can be considered as a finite-size Hamiltonian that contains the finite bulk surrounded by two bath sites. The matrix representation of  $\hat{\mathcal{H}}$  in local basis is exactly  $\mathcal{H}$  in Eq. (S9).

What is more interesting is that  $\hat{\mathcal{H}}$  is formed by the original Hamiltonian in the bulk  $\tilde{H}_B$  as well as two Hamiltonians on the boundary of the bulk as

$$\hat{\mathcal{H}} = \hat{\mathcal{H}}_L \tilde{H}_B \hat{\mathcal{H}}_R, \quad (\text{S12})$$

where the Hamiltonians  $\hat{\mathcal{H}}_L$  and  $\hat{\mathcal{H}}_R$  on the boundaries satisfy

$$\begin{aligned} \langle bs | \hat{\mathcal{H}}_L | b' s' \rangle &= \sum_a V_{ab_1 b'_1}^L \langle s | \hat{F}_R(s, a)^\dagger | s' \rangle, \\ \langle sb | \hat{\mathcal{H}}_R | s' b' \rangle &= \sum_a \langle s | \hat{F}_L(s, a)^\dagger | s' \rangle V_{ab_1 b'_1}^R, \end{aligned} \quad (\text{S13})$$

$\hat{\mathcal{H}}_L$  and  $\hat{\mathcal{H}}_R$  are just two-body Hamiltonians between the bath site and the physical site on the boundary of the bulk.

Ref. [13] shows that  $\hat{\mathcal{H}}_L$  and  $\hat{\mathcal{H}}_R$  can be written in a shifted form as

$$\hat{\mathcal{H}}_{L(R)} = I - \tau \hat{H}_{L(R)}. \quad (\text{S14})$$

$\hat{H}_{L(R)}$  is independent on  $\tau$  and called the physical-bath Hamiltonian. Then  $\hat{\mathcal{H}}$  can be written as the shift of a few-body Hamiltonian as  $\hat{\mathcal{H}} = I - \tau \hat{H}_{FB}$ , where  $\hat{H}_{FB}$  has the standard summation form as

$$\hat{H}_{FB} = \hat{H}_L + \sum_{n=1}^L \hat{H}_{n,n+1} + \hat{H}_R. \quad (\text{S15})$$

$\hat{H}_{FB}$  is the few-body Hamiltonian that optimally mimics the ground state of the infinite system.  $\hat{H}_L$  and  $\hat{H}_R$  are the tuning Hamiltonian employed in the CSW.

After obtaining  $\hat{H}_L$  and  $\hat{H}_R$  by solving the self-consistent equations in Eqs. (S6) - (S9), the next step is calculating the coupling constants and magnetic fields. If one takes the bond (bath) dimension to be  $\chi$ ,  $\hat{H}_{L(R)}$  is a  $(2\chi \times 2\chi)$  matrix. The Hamiltonian represents the interaction between a spin-1/2 and a bath site. Then  $\hat{H}_{L(R)}$  can be generally expanded by  $\hat{S}^{\alpha_1} \otimes \hat{S}^{\alpha_2}$  with  $\{\hat{S}\}$  the generators of the  $SU(\chi)$  group.

In our case, we take the bond dimension  $\chi = 2$ , and  $\hat{H}_{L(R)}$  just gives the Hamiltonian between two spin-1/2's. Thus, it can be expanded by  $\hat{S}^{\alpha_1} \otimes \hat{S}^{\alpha_2}$ , as

$$\hat{H}_{L(R)} = \sum_{\alpha_1, \alpha_2=0}^3 J_{L(R)}^{\alpha_1 \alpha_2} \hat{S}^{\alpha_1} \otimes \hat{S}^{\alpha_2}, \quad (\text{S16})$$

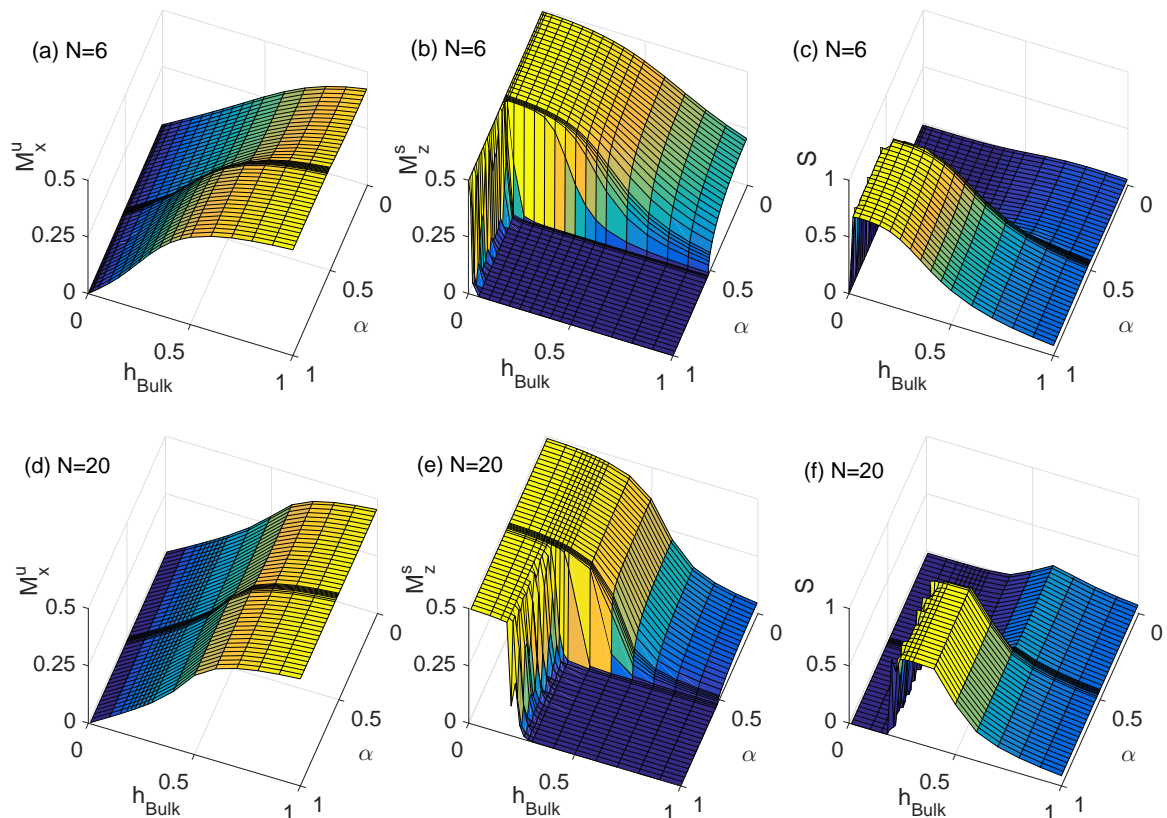


Figure S1: (Color online) (a)-(c) show the ground-state uniform magnetization in the x direction  $M_x^u$ , staggered magnetization in the z direction  $M_z^s$  and the entanglement entropy  $S$  with different values of the bulk transverse field  $h_{\text{Bulk}}$  and the control parameter  $\alpha$  of the TH's on the boundaries. We take the system  $N = 6$ . (d)-(f) show the same quantities with  $N = 32$ . For different system sizes, the switch point remains at  $\alpha^s = 0.5$ , and the landscapes for  $\alpha < 0.5$  do not change much. For  $\alpha > 0.5$ , the boundary of the Néel phase and polarized phase moves.

where the spin-1/2 operators are labeled as  $\hat{S}^0 = I$ ,  $\hat{S}^1 = \hat{S}^x$ ,  $\hat{S}^2 = \hat{S}^y$ , and  $\hat{S}^3 = \hat{S}^z$ . Then with  $\alpha_1 \neq 0$  and  $\alpha_2 \neq 0$ , we have  $J_{L(R)}^{\alpha_1 \alpha_2}$  as the coupling constants, and  $J_{L(R)}^{\alpha_1 0}$  and  $J_{L(R)}^{0 \alpha_2}$  the magnetic fields on the first and second sites, respectively.  $J_{L(R)}^{00}$  only provides a constant shift of the Hamiltonian which does not change the eigenstates.

#### SUPPLEMENTARY RESULTS: SIZE-DEPENDENCE, COUPLING STRENGTH, FIDELITY, AND THE CONTROLLING BY LOCAL MAGNETIC FIELDS

**Size dependence.** We calculate the ground-state uniform magnetization in spin-x direction  $M_x^u$ , staggered magnetization in spin-z direction  $M_z^s$  and the entanglement entropy  $S$  for  $N = 6$  and  $N = 32$  (Fig. S1).

For both sizes, the switch point stays at  $\alpha^s = 0.5$ . This is expected because the switch should be triggered by the entanglement bath provided by the TH's. The landscapes of the quantities for  $\alpha < 0.5$  do not exhibit drastic changes, only with quantitative differences between  $N = 6$  and  $N = 32$ . Differently, we show that the boundary between the Néel phase and the polarized phase moves as  $N$  changes for  $\alpha > 0.5$ . With  $N = 6$ , the width of the Néel phase very narrow, where the location of the cliff of  $M_z^s$  and the peak of  $S$  is quite close to zero at  $\alpha \approx O(10^{-3})$ . For  $N = 32$ , the width is much larger, and the cliff of  $M_z^s$  and the peak of  $S$  appear at  $\alpha \approx 0.28$ .

In Fig. S2, we calculate  $M_z^s$  at  $\alpha = 1$  for different sizes  $N$ . The yellow area shows the Néel region, whose width increases with  $N$ . In theory, the width will approach to  $h_{\text{Bulk}} = 0.5$  for  $N \rightarrow \infty$ , where we have the infinite quantum Ising chain and the quantum phase transition occurs at  $h_{\text{Bulk}} = 0.5$ . Compared with the finite quantum Ising chain without the TH's, the positions of the cliffs of  $h_{\text{Bulk}} = 0.5$  are given by the red crosses. The differences between the CSW and the finite Ising chain is only quantitative, around  $O(10^{-2})$ .

**Coupling strength dependence.** How strong need the TH's be to activate the switch? Our results amazingly show that only a

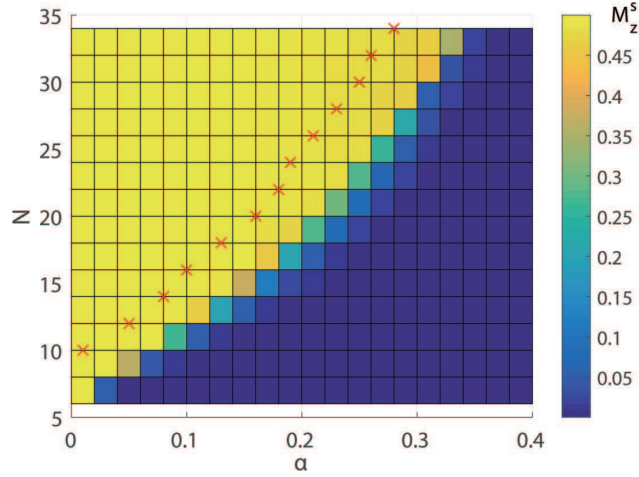


Figure S2: (Color online) The staggered magnetization  $M_z^s$  of the CSW with the TH's for different sizes  $N$  at  $\alpha = 1$ . The width of the Néel phase increases with  $N$ . The red crosses gives the positions of the cliffs without the TH's, where  $M_z^s$  drops rapidly and the ground state start entering the polarized phase from the Néel phase. The differences of the positions with or without the TH's are about  $\Delta h_{Bulk} \sim O(10^{-2})$ .

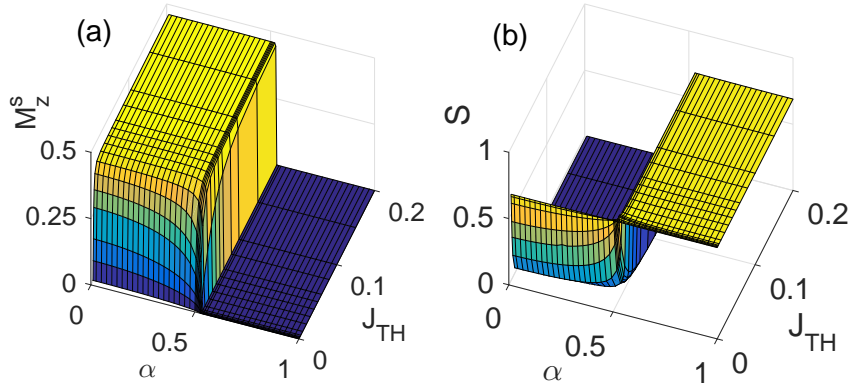


Figure S3: (Color online) The ground-state uniform magnetization in spin-x direction  $M_x^u$ , staggered magnetization in spin-z direction  $M_z^s$  and the entanglement entropy  $S$  in the middle of the chain with different values of TH coupling strength  $J_{TH}$  and the control parameter  $\alpha$ . We fix  $h_{Bulk} = 0.3$  and  $N = 12$ . The switch of the landscape is induced by a very small TH coupling strength of  $J_{TH} \sim O(10^{-2})$ .

very weak strength of the TH's is needed. To control the coupling strength of the TH's, we add a constant  $J_{TH}$  in Eq. (1) as

$$\hat{H} = \hat{H}_{Bulk} + J_{TH}(\hat{H}_L + \hat{H}_R). \quad (S17)$$

Note that we have the  $(N - 2)$ -site transversing Ising chain for  $J_{TH} = 0$ , and the Hamiltonian in Eq. (1) for  $J_{TH} = 1$ .

As shown in Fig. 3, when we fix  $h_{Bulk} = 0.3$  and tune  $\alpha$ , there will be a drastic change of  $M_z^s$  and  $S$  of the CSW that indicates the switch point of the landscape with the TH's. The results with different  $J_{TH}$  are shown in Fig. S3. By changing  $J_{TH}$  and  $\alpha$ ,  $M_x^u$  almost keeps unchanged, which is expected according to the results above. For  $M_z^s$  and  $S$ , the switch of the landscape behavior start to appear as soon as the  $J_{TH}$  becomes non-zero, and is completely turned on as Fig. 3 only with  $J_{TH} \sim O(10^{-2})$ . These results show that one only needs a very small coupling strength of the TH's to induce the switch of the landscapes.

**Controlling by the local magnetic fields.** We find that the controlling can be activated/deactivated by simply tuning the magnetic fields  $h_2$  at the second and last second sites (Fig. S4). The Hamiltonian reads

$$\hat{H} = \sum_{n=2}^{N-2} \hat{S}_n^z \hat{S}_{n+1}^z + \hat{H}_L + \hat{H}_R - h_2(\hat{S}_2^x + \hat{S}_{N-1}^x) - h_{Bulk} \sum_{n=3}^{N-2} \hat{S}_n^x. \quad (S18)$$

For  $h_2 = 0$ , the change of  $\alpha$  has nearly no effects on the bulk, meaning the controlling is deactivated in this case. By increasing  $h_2 \neq 0$ , one can see that the controlling appears as soon as  $h_2$  becomes non-zero, and is fully activated at  $h_2 \sim O(10^{-2})$ .

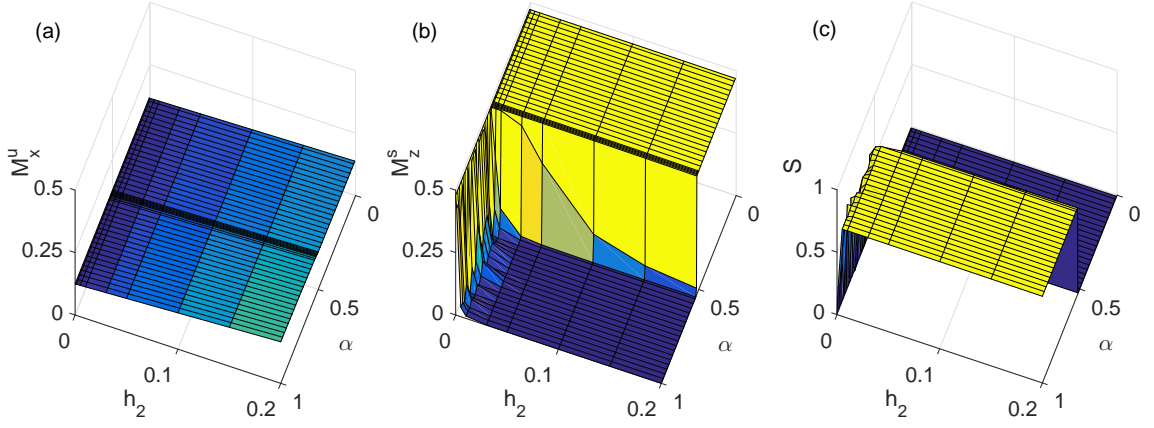


Figure S4: (Color online) The ground-state uniform magnetization in spin-x direction  $M_x^u$ , staggered magnetization in spin-z direction  $M_z^s$  and the entanglement entropy  $S$  with different  $\alpha$  and  $h_2$  that is the transverse magnetic on the second and last second sites. For  $h_2 = 0$ , the change of  $\alpha$  has nearly zero effects on the bulk, meaning the controlling is deactivated in this case. With a nonzero  $h_2$ , the controlling appears, indicating by a steep change of  $M_z^s$  and  $S$  around  $\alpha = 0.5$ . Here we take  $N = 12$  and  $h_{Bulk} = 0.3$  [Eq. (S18)].

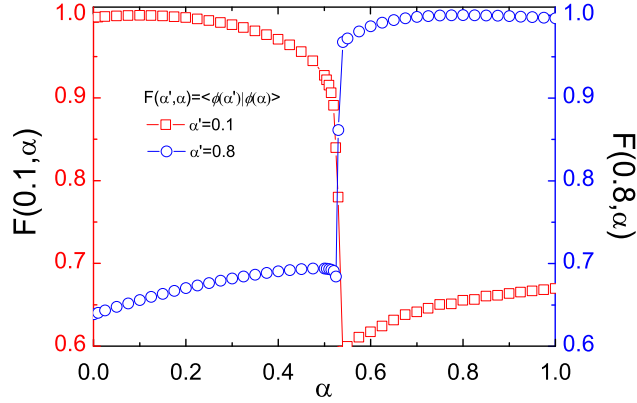


Figure S5: (Color online) The ground state fidelity  $F(0.1, \alpha)$  and  $F(0.8, \alpha)$  of the CSW as the function of the control parameter  $\alpha$ . We fix  $h_{Bulk} = 0.3$  and  $N = 18$ .

**Fidelity in the controlling.** We also investigate the fidelity  $F(\alpha', \alpha)$  defined as

$$F(\alpha', \alpha) = |\langle \phi(\alpha') | \phi(\alpha) \rangle|. \quad (S19)$$

Here,  $|\phi(\alpha)\rangle$  is the ground state of the CSW with the control parameter taken as  $\alpha$ . We choose the size to be  $N = 18$  and the magnetic field  $h_{Bulk} = 0.3$  in the bulk. Note that the signs of  $\bar{h}_x$  and  $\bar{J}_{zz}$  can be taken freely, we fix them to be positive.

Fig. S5 shows the curves of  $F(\alpha', \alpha)$  at  $\alpha' = 0.1$  and  $0.8$ . The maximum of  $F(\alpha', \alpha)$  is very close to 1, which is expected when  $\alpha' \simeq \alpha$ . When  $\alpha$  and  $\alpha'$  locate on two different sides of the switch point  $\alpha^s = 0.5$ , the fidelity drops. The minimum is  $F(\alpha', \alpha) \simeq 0.6 \gg 0$ , meaning the polarized states and the Néel states are not orthogonal to each other. A drastic change occurs at the switch point, which is consistent with the results of other quantities such as energies, magnetizations and entanglement spectrum/entropy.

**Spectrums without the tuning Hamiltonians.** For comparison, Fig. S6 shows the energy spectrum and entanglement spectrum for the pure quantum Ising chain with no TH's on the boundaries. By tuning  $\alpha$  (the magnetic fields on the boundary sites), we find no non-trivial changes of the degeneracy of the ground state or dominant Schmidt numbers.

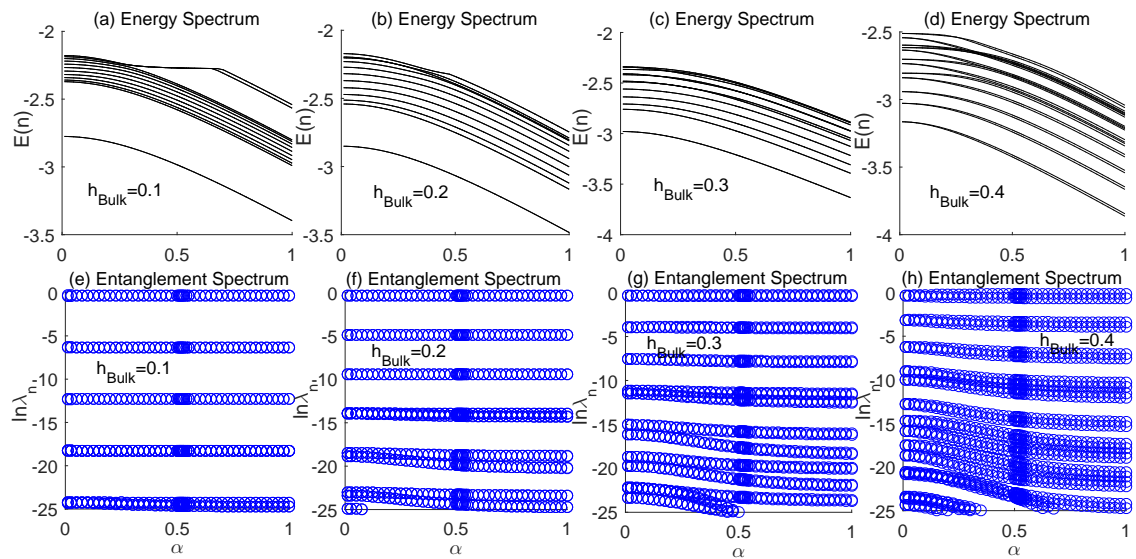


Figure S6: (Color online) The  $\alpha$ -dependence of (a)-(d) the energy spectrum and (e)-(h) the entanglement spectrum in the middle of the finite quantum Ising chain without the TH's. In this case, the spectrums show different structure when varying  $\alpha$ , compared with Fig. 2.